COMPUTATIONAL CONTINUUM MECHANICS

ВЫЧИСЛИТЕЛЬНАЯ МЕХАНИКА СЛОШНЫХ СРЕД

Computational Continuum Mechanics. 2021. Vol. 14. No. 2. pp. 127-143 DOI: 10.7242/1999-6691/2021.14.2.11

SOME RESULTS OF NUMERICAL ESTIMATING THE STABILITY OF THE FCC METAL TWO-LEVEL CONSTITUTIVE MODEL

A.I. Shveykin, P.V. Trusov, K.A. Romanov

Perm National Research Polytechnic University, Perm, Russian Federation

An important property of constitutive models is the stability of the response change histories obtained under various perturbations of an input data (history of influences and initial conditions) and a model operator. It is associated with the stochastic nature of material properties at different structural-scale levels and thermomechanical influences. Stability analysis is especially significant to justify the applicability of new constitutive models for describing modern technological processes, for instance, those focused on the design of novel functional materials. Multilevel physically-oriented constitutive models of materials hold the most promise for solving such problems. They are able to provide an explicit description of the inelastic deformation mechanisms, the material structure rebuilding and the changes in the physical and mechanical properties of the material determined by its state. The approach developed by the authors and described in detail in the paper in the previous issue of the journal made it possible to evaluate the stability of multilevel constitutive material models under various perturbations of the initial conditions, the history of influences, and parametric operator perturbations. It includes the analysis of the norms of their deviations and the integral norm of deviation of perturbed solutions from the basic ones obtained in calculations with unperturbed parameters. In this paper, the application of the proposed approach has been illustrated by studying the two-level constitutive model of the FCC polycrystal. The obtained results demonstrate the stability of this model to the calculated perturbations.

Key words: multilevel constitutive model, mathematical model stability, sensitivity to perturbation

1. Introduction

In recent decades, a multilevel approach to the construction of constitutive models (CMs) for metals and alloys, based on the introduction of internal variables (IV) and physical theories of plasticity, has been intensively developed [1–7]. These models give the possibility to explicitly describe the material structure evolution and changes in the physical and mechanical macroproperties (including anisotropic) of materials, as well as the mechanisms responsible for deformation of these materials. Therefore, they are frequently used to investigate and improve the metal processing and forming techniques, as well as to solve the problems aimed at developing new functional materials.

In multilevel models [8, 9], memory characteristics of inelastically deformed solids are taken into account by introducing IVs. Besides, the application of IVs that characterize the current state of the structure and implementation of any deformation mechanisms at different structural-scale level [5, 10, 11] makes it possible to avoid the use of sophisticated integral operators with properties similar to material memory characteristics (the memory is stored in the values of IVs). So, the multilevel CMs of this type are, in the general case, the algorithmic operator equations, involving systems of differential and/or tensor-algebraic equations [5, 10, 11–16]. When the structure evolution, main deformation mechanisms and interactions between these mechanisms are properly described, the models (and submodels introduced to characterize changes in individual structural elements and specific deformation mechanisms) demonstrate significant versatility, which provides a wide range of their applications. Since many mechanisms in deformable solids are realized and interact at various structural-scale levels, the versatility of CMs, in particular, their efficiency under various loading conditions, including complex loading, can be achieved by introducing a large number of IVs and kinetic (as a rule, nonlinear) equations.

An arbitrary mathematical model can be represented as an operator that allows to find the *output data (solution)* by employing the *input data* that contains, in the general case, time-varying influences on the object of research and initial conditions [17]. An essential attribute of the analysis

Email addresses for correspondence: shveykin@pstu.ru

of complex models involves examining the stability of the solutions obtained using these models in relation to input and operator perturbations. The relevance of these manipulations for CMs is due to the fact that both material properties (distributed over the construction at different structural-scale levels)and influences (distributed over the examined area and its boundaries) produced by stochastic boundary conditions are of stochastic nature.

The analysis of stability is often associated with the need for assessment of the sensitivity of the CM response to the parameters that characterize the physical and mechanical properties of the material [18-22]. It is expedient for the CM identification procedure [23-26]: if there is high sensitivity to material parameters (weakly perturbed at the values established during the identification procedure), then the domain of their definition seems to be revised with regard to physical considerations. The results of the analysis of sensitivity of the multilevel CM response to the perturbations of some parameters, in particular, the values of constants used in kinetic equations and the initial values of internal variables, previously obtained by the authors, are discussed in [27]. Note that the analysis of sensitivity can be considered a special case of the analyzing the stability of the model under parametric perturbations of the CM operator [28].

In [28], describing an approach to the numerical assessment of the stability of multilevel constitutive models of inelastic behavior of metals and alloys, the analysis of the mathematical structure of multilevel CMs, represented as a system of ordinary differential and algebraic equations with an algebraic definition of the right-hand part, is considered. It was shown that, although the Lyapunov's methods are successfully applied for solving different partial stability analysis problems (e.g., in [34-37]), there are seemingly insurmountable difficulties associated with high nonlinearity and dimensionality of systems equations in applying these methods to multilevel CMs. The authors of [28] formulated a generalized definition of *stability of the solution* which, unlike the traditional one, takes into account perturbations of history of influences and the parametric perturbations of operator; a program of computational experiments to implement the proposed approach is also presented, which includes the assignment of various perturbations of the initial conditions, history of influences and operator and the calculation of the norms of deviation of the perturbed solutions from the base ones. The *procedure for assessing the stability of the model* is understood as the analysis of the stability of solutions for different values of the parameters (determined in multiple subsets of the domain of their definition) that specify the operator and input data (initial conditions and influences), i.e., consideration of some problems of assessment of the local stability of the model. If the unstable solution (mathematically induced instability) is established, then it is necessary to clarify whether the mathematically induced instability is physically induced [28].

In this paper, the application of the proposed approach is demonstrated by the case of studying a two-level constitutive model for describing the deformation of a FCC polycrystal. Section 2 contains the correlations for the constitutive model. Section 3 describes a program for the numerical implementation of the approach step by step and analyzes the results obtained.

2. Two-level constitutive model of the FCC polycrystal

In two-level statistical models based on theories of crystal plasticity, a sample of crystallites, the deformation of which is assumed to be homogeneous, is associated with a representative volume of a polycrystalline material at the macrolevel [5, 38–40]. At present, statistical models are mainly used for modeling of technological processes of thermomechanical treatment due to the fact that self-consistent [4, 41] and direct models, implying the determination of inhomogeneous fields at the meso-level [2,3], are much more resource-intensive.

The system of equations at a macroscale level can be written as (hereinafter, the macroscale quantities are denoted by capital letters, and similar quantities of a meso-level, i.e., a crystallite level, by the same lower-case letters; to shorten the notation, the crystallite index is omitted)

$$\mathbf{K}^{\mathrm{cor}} \equiv d\mathbf{K}/dt - \bar{\mathbf{\Omega}}\cdot\mathbf{K} + \mathbf{K}\cdot\bar{\mathbf{\Omega}} = \bar{\mathbf{\Pi}} : \left(\mathbf{L} - \bar{\mathbf{\Omega}} - \mathbf{Z}^{\mathrm{in}}\right), \qquad 1 \quad (1)$$

$$\bar{\mathbf{\Omega}} = \left\langle \bar{\boldsymbol{\omega}} \right\rangle, \qquad 2$$

$$\bar{\mathbf{\Pi}} = \left\langle \bar{\boldsymbol{\pi}} \right\rangle, \qquad 3$$

$$\mathbf{Z}^{\text{in}} = \left\langle \mathbf{z}^{\text{in}} \right\rangle + \bar{\mathbf{\Pi}}^{-1} : \left\langle \bar{\boldsymbol{\pi}}' : \left(\mathbf{z}^{\text{in}} \right)' \right\rangle + \bar{\mathbf{\Pi}}^{-1} : \left(\left\langle \boldsymbol{\kappa}' \cdot \bar{\boldsymbol{\omega}}' \right\rangle - \left\langle \bar{\boldsymbol{\omega}}' \cdot \boldsymbol{\kappa}' \right\rangle \right). \qquad 4$$

The constitutive equation $(1)_1$ is expressed in terms of the current configuration; $\mathbf{K}$ is the weighted Kirchhoff stress tensor at the macrolevel; $\mathbf{K} = \left\langle \overset{\circ}{\rho} / \hat{\rho} \right\rangle \mathbf{\Sigma}$, where $\langle \cdot \rangle$ stands for averaging over a representative macro volume, $\mathbf{\Sigma}$ is the Cauchy stress tensor at the macro level; $\overset{\circ}{\rho} / \hat{\rho}$ is the density ratio in the initial and current configurations for the crystallites included in the representative macro level volume (according to the Taylor hypothesis, $\overset{\circ}{\rho} / \hat{\rho}$ ratios are equal in all crystallites); $\mathbf{K}^{\text{cor}} \equiv d\mathbf{K}/dt - \bar{\mathbf{\Omega}} \cdot \mathbf{K} + \mathbf{K} \cdot \bar{\mathbf{\Omega}}$ is the corotational rate of change of the weighted Kirchhoff stress tensor, which is independent of choice of reference frame; the kinematic influence is set by the velocity gradient at the macro level, $\mathbf{L} = \hat{\nabla} \mathbf{V}^{\text{T}}$.

During the procedure of averaging over the representative macrovolume (the average by the sample of crystallites), the moving coordinate system spin tensor $\bar{\mathbf{\Omega}}$ (relation $(1)_2$) and the elastic property tensor $\bar{\mathbf{\Pi}}$ (relation $(1)_3$) are transferred from the mesolevel model to the macrolevel. The inelastic strain rate tensor $\mathbf{Z}^{\text{in}}$ is determined in terms of the meso-level model via matching the macro level and meso-level constitutive relation [42] (to ensure the equality of macrostresses and averaged mesostresses: $\mathbf{K} = \langle \boldsymbol{\kappa} \rangle$); $\mathbf{a}'$ is the deviation of the tensor characteristic $\mathbf{a}$ for an individual crystallite from the mean (for the representative macrovolume) value; $\mathbf{a}' = \mathbf{a} - \langle \mathbf{a} \rangle$ (the averaging operation has the property $\langle \mathbf{a}' \rangle = \mathbf{0}$ for each $\mathbf{a}$).

The structure of the model (1) reflects the capabilities of multilevel models for considering macrolevel parameters as effective quantities that integrally characterize the deformation processes realized at the mesolevel. In particular, the issue of determining the corotational derivative is resolved which is important in constructing models for describing technological processes with large velocity gradients (geometric nonlinearity) [43–49]. For this purpose, it is essential to get information on the moving coordinate systems of individual crystallites, which are connected with the symmetry elements of crystallites [5]. Note that a change in the material symmetry at the macrolevel due to texture formation does not require constitutive model refinement. In [50–52], the application of the proposed approach to formulating geometrically nonlinear relations was justified. It was shown that, at small elastic deformations characteristic of metals and alloys, the model gives results close to those obtained in alternative mesoscale models, including the most popular form of constitutive relations in terms of the unloaded configuration (see [2, 4, 53], etc.). Meanwhile, the rate-type CMs in the actual configuration are more adapted to numerical methods for solving boundary value problems used to study thermomechanical processes; the configuration of the computational domain, including the contact surfaces with the tool, needs to be redefined. Another advantage of this formulation is the possibility of an additive decomposition of the inelastic strain rate into contributions of various mechanisms, which greatly facilitates the development of the corresponding CMs. Examples of the constitutive models proposed by the authors of this work for studying, in particular, grain boundary sliding effects are given in [5, 54, 55].

For each crystallite, we use the meso-level system of equations (to shorten the writing of formulas, the crystallite index is omitted) [5]

$$\boldsymbol{\kappa}^{\text{cor}} \equiv d\boldsymbol{\kappa}/dt + \boldsymbol{\kappa} \cdot \bar{\boldsymbol{\omega}} - \bar{\boldsymbol{\omega}} \cdot \boldsymbol{\kappa} = \bar{\boldsymbol{\pi}} : \left(\mathbf{l} - \bar{\boldsymbol{\omega}} - \sum_{k=1}^{K} \dot{\gamma}^{(k)} \mathbf{b}^{(k)} \mathbf{n}^{(k)} \right), \qquad 1 \qquad (2)$$

$$\dot{\gamma}^{(k)} = \dot{\gamma}_0 \left(\tau^{(k)} / \tau_c^{(k)} \right)^{\mathrm{m}} H(\tau^{(k)} - \tau_c^{(k)}) \quad (k = 1, ..., K), \qquad 2$$

$$\tau^{(k)} = \boldsymbol{\kappa} : \mathbf{b}^{(k)} \mathbf{n}^{(k)} \quad (k = 1, ..., K), \qquad 3$$

$$\dot{\tau}_{\mathrm{c}}^{(k)} = \left[\text{Equations for determining } \dot{\tau}_{\mathrm{c}}^{(k)} \right] \quad (k = 1, ..., K), \qquad 4$$

$$\bar{\boldsymbol{\omega}} = \left[\text{Equations for determining } \bar{\boldsymbol{\omega}} \right], \quad \dot{\mathbf{o}} \cdot \mathbf{o}^{\mathrm{T}} = \bar{\boldsymbol{\omega}}. \qquad 5$$

In (2), $\boldsymbol{\kappa} = \left(\overset{\circ}{\rho} / \hat{\rho} \right) \boldsymbol{\sigma}$ is the weighted Kirchhoff stress tensor at the meso-level, where $\boldsymbol{\sigma}$ is the Cauchy stress tensor at the meso-level; $\bar{\boldsymbol{\omega}}$ is the spin of a moving coordinate system related to the lattice [50]; $\bar{\mathbf{n}}$ is the elastic property tensor (its components are constant in the moving coordinate system); $\mathbf{l} = \hat{\nabla} \mathbf{v}^{\mathrm{T}}$ is the velocity gradient (according to the Taylor hypothesis, $\mathbf{l} = \hat{\nabla} \mathbf{v}^{\mathrm{T}} = \hat{\nabla} \mathbf{V}^{\mathrm{T}} = \mathbf{L}$, where $\hat{\nabla} \mathbf{V}^{\mathrm{T}}$ is taken at the macro level); $\dot{\gamma}^{(k)}$, $\mathbf{b}^{(k)}$, $\mathbf{n}^{(k)}$ are the shear rates, unit vectors of slip direction and slip plane normal (in the actual configuration) of edge dislocations for the slip system k; K is the number of crystallographic slip systems (a doubled number of slip systems $K = 24$ is used for FCC lattice). The dot above the symbol denotes the time derivative of the corresponding quantity. The inelastic strain rate tensor is defined at the meso-level as $\mathbf{z}^{\mathrm{in}} = \sum_{k=1}^{K} \dot{\gamma}^{(k)} \mathbf{b}^{(k)} \mathbf{n}^{(k)}$.

The values $\dot{\gamma}^{(k)}$ on the slip systems are calculated using the viscoplastic relationship $(2)_2$, where $\tau^{(k)}, \tau_{\mathrm{c}}^{(k)}$ are, respectively, shear and critical shear stresses for the slip system k; $\dot{\gamma}_0$ is the shear rate for the slip system k when the shear stress reaches its critical value; m is the strain rate sensitivity exponent; $H(\cdot)$ is the Heaviside function.

The formulation of the hardening law – kinetic equations (2_4) for critical shear stresses $\tau_c^{(k)}$ — has been the subject of many studies devoted to the development of theories of crystal plasticity (the approaches proposed in [56–59] are the most popular ones; a comprehensive review of papers published on this theme in recent decades is given in [5]). Such interest is explained by the fact that it is precisely these $\tau_c^{(k)}$ (internal variables) that characterize the resistance of the lattice and defect structure to dislocation motion. Therefore, the change of these variables must be associated with a change in the defect structure. Since in this article we propose to focus on the procedure for assessing the stability of the model, then a fairly simple and well-known hardening law of the form [53, 60] is used in the calculations, which can be written as

$$\dot{\tau}_{\mathrm{c}}^{(k)} = \sum_{l=1}^{\mathrm{K}} h^{(kl)} (\boldsymbol{\sigma}) \dot{\gamma}^{(l)}, \quad h^{(kl)} = \left[q_{\mathrm{lat}} + (1 - q_{\mathrm{lat}}) \delta^{(kl)} \right] h^{(l)}, \quad h^{(l)} = \mathrm{h}_0 \left| 1 - \tau_{\mathrm{c}}^{(l)} / \tau_{\mathrm{sat}} \right|^{\mathrm{a}}, \qquad (3)$$

where the latent hardening parameter q_{lat} and its value is taken as 1.0 for coplanar slip systems and as 1.4 for noncoplanar slip systems (with numbers k and l), $\delta^{(kl)}$ is the Kronecker delta, τ_{sat} is the so-called saturation stress [53, 60], and the parameters h_0, a are determined from the experimental data.

The movable coordinate system is assocoated with the crystallographic axes [5]. In this case, the tensors included in the CM formulation will be indifferent for the observer in a fixed laboratory coordinate system, which makes it possible to follow the principle of independence of the constitutive relation of choice of reference frame to be fulfilled [8]. To calculate the spin (2_5), we use the following equation [50]:

$$\overline{\boldsymbol{\omega}} = \dot{\mathbf{k}}_i \mathbf{k}_i = -\left(\mathbf{k}_2 \cdot \mathbf{l}^{\mathrm{e}} \cdot \mathbf{k}_1\right)\mathbf{k}_1\mathbf{k}_2 - \left(\mathbf{k}_3 \cdot \mathbf{l}^{\mathrm{e}} \cdot \mathbf{k}_1\right)\mathbf{k}_1\mathbf{k}_3 + \left(\mathbf{k}_2 \cdot \mathbf{l}^{\mathrm{e}} \cdot \mathbf{k}_1\right)\mathbf{k}_2\mathbf{k}_1 - \\ -\left(\mathbf{k}_3 \cdot \mathbf{l}^{\mathrm{e}} \cdot \mathbf{k}_2\right)\mathbf{k}_2\mathbf{k}_3 + \left(\mathbf{k}_3 \cdot \mathbf{l}^{\mathrm{e}} \cdot \mathbf{k}_1\right)\mathbf{k}_3\mathbf{k}_1 + \left(\mathbf{k}_3 \cdot \mathbf{l}^{\mathrm{e}} \cdot \mathbf{k}_2\right)\mathbf{k}_3\mathbf{k}, \qquad (4)$$

where $\mathbf{k}_i$ is the orthonormal basis of the moving coordinate system, the orientation of which relative to the fixed laboratory system is defined by the proper orthogonal tensor $\mathbf{o}$, $\mathbf{l}^{\mathrm{e}} = \mathbf{l} - \sum_{k=1}^{K} \dot{\gamma}^{(k)} \mathbf{b}^{(k)} \mathbf{n}^{(k)}$ is the elastic component of the velocity gradient. In deriving (4), we have taken into account the invariance of the lattice (and, hence, of the moving coordinate system) under plastic deformation due to the motion of edge dislocations along the slip systems [50].

In the numerical calculations we considered a representative volume of a polycrystal with a face-centered cubic lattice (hereinafter referred to as an FCC polycrystal) using a statistical model. The volume included a sample of 343 crystallites, the initial orientations of which were distributed randomly according to a uniform law. The nominal properties of the polycrystal corresponded to those of copper. The meso-level elastic property tensor contained the following independent components (constant for the observer in a rigid moving coordinate system linked with the lattice): $\text{п}_{1111} = 168{,}4$ GPa, $\text{п}_{1122} = 121{,}4$ GPa, $\text{п}_{1212} = 75{,}4$ GPa [61]; the viscoplastic relationship included $\dot{\gamma}_0 = 0{,}001$ c^{-1}, $1/\text{m} = 0{,}012$; the hardening law parameters were $\text{h}_0 = 180$ MPa, $\text{a} = 2{,}25$, $\tau_{\text{sat}} = 148$ MPa, and the initial values of critical stresses for all slip systems were $\tau_{\text{c}}^{(k)}(0) = \tau_{\text{c}0} = 16$ MPa ($k = 1, \ldots, K$) [53, 60].

The CM given above was represented as a system of algebraic and ordinary differential equations. Due to the significant nonlinearity of the system of equations, in particular, the presence of the Heaviside function in the viscoplastic law $(2)_2$ (which led to the necessity of discretization with a small time step to trace the activity of slip systems in crystallites; in the calculations, the time step was 0.002 s), these equations were integrated using an explicit Euler method.

Figure 1 shows the dependences of the components $(-\Sigma_{33})$ and $(-\Sigma_{23})$ in the orthonormal laboratory coordinate system (LCS) with a basis $\mathbf{p}_i$ (where $i = \overline{1,3}$) of the Cauchy stress tensor at the macrolevel on the logarithmic strain component $(-H_{33})$ under uniaxial compression and on the shear value under simple shear, respectively. Note that, although the parameters used in the calculations were determined during their identification in compression phase [60], the results of changes in shear stresses at simple shear (used for verification) were found to be in good agreement with the experimental data.

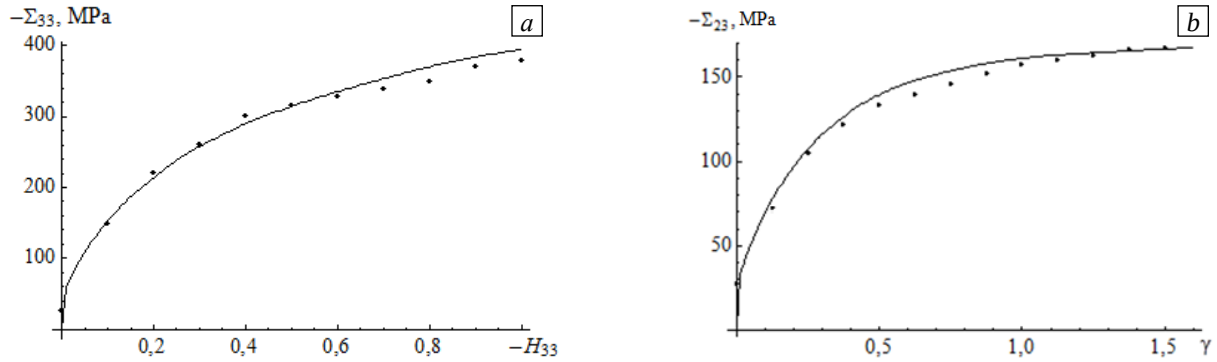

Fig.1. Dependence of $(-\Sigma_{33})$ on H_{33} under uniaxial compression (*a*) and dependence of $(-\Sigma_{23})$ on shear value under simple shear (b); dots are the experimental data from [60], and solid line are the results obtained using the proposed model.

The paper [27] presents the results illustrating the application of the proposed CM for describing simple and complex loading modes and the estimates of its sensitivity to the perturbations of some

characteristics: viscoplastic law parameters $\dot{\gamma}_0$, m; hardening law parameters h_0, a, τ_{sat}; initial values of critical stresses for all slip systems τ_{c0}. The data obtained indicate the stability of CMs with respect to changes in these parameters. The parameters were ranked according to their degree of sensitivity; it was found that the deviation of the parameter τ_{sat} has the greatest effect on the output data.

On the basis of the approach to the analysis of stability proposed in [28], it can be concluded that the study of the influence of perturbations of the initial values of critical stresses τ_{c0} refers to the case of initial conditions perturbations due to IVs, and the study of the perturbations of the remaining parameters – to parametric perturbations of operator. Below, we present a step-by-step description of the implementation of computations in accordance with the approach under discussion. For this purpose, we consider the CM described and evaluate a wider set of perturbed parameters.

3. The results of application of the technique for studying the stability in relation to perturbations of influences and parametric perturbations of operator

In the framework of the notion system from [28],

– the vector of influence $\mathbf{X}=\{L_{ij}(t)\}$ $(i,j=\overline{1,3})$, $t\in[0,T]$ is defined in terms of $L_{ij}(t)$— components of the velocity gradient tensor in LCS;

– the output data $\mathbf{Y}=\{\Sigma_{ij}(t)\}$ $(i,j=\overline{1,3})$, $t\in[0,T]$ is defined in terms of $\Sigma_{ij}(t)$ — components of the macrolevel Cauchy stress tensor in LCS;

– the vector of internal variables **Z** is defined as composed of the previously introduced (for each grain of the sample) mesostress components, components of the orientation tensor of a crystallographic coordinate system, shears on the slip systems and critical stresses associated with their activation (no information is provided on the perturbations of IV initial values because of the limited size of this paper; some data can be found in [27]).

Numerical implementation of the approach to studying the stability of CMs under specified loads includes the following steps [28]:

STEP 1. Definition of base solutions

Base solutions are the solutions without any parameter perturbations. They were compared with the solutions obtained in various implementations under random perturbations of some parameters (according to the prescribed program of numerical experiments, see STEP 3); other parameters were not perturbed.

As base solutions, the solutions obtained for the representative volume under the following isothermal rigid loading modes were considered:

1) Kinematic loading with the velocity gradient $\mathbf{L}(t)=(\dot{\varepsilon}/2)(\mathbf{p}_1\mathbf{p}_1+\mathbf{p}_2\mathbf{p}_2)-\dot{\varepsilon}\,\mathbf{p}_3\mathbf{p}_3$. The base solutions determined using CMs for some perturbations are given in Fig.4. Note that, in [60] this loading was applied to a statistic CM as an approximation of uniaxial compression (for the sake of shortness, we call it “quasi-compression”).

2) Simple shear $\mathbf{L}(t)=-\dot{\varepsilon}\,\mathbf{p}_2\mathbf{p}_3$.

In both rigid loading modes, $\dot{\varepsilon}=0,001$ s^{-1}, and the deformation develops in the time interval $0\le t\le T$, where $T=1000$ s.

STEP 2. Setting the influence and operator perturbations

The paper [27] presents the results of a study of the sensitivity of the response to changes in the numerical values of some characteristics of the operator (the viscoplastic law parameters and hardening law parameters) and in the initial conditions (the initial values of critical shear stresses in slip systems). The data obtained indicate the response resistance to the corresponding perturbations.

Further, it seems reasonable to analyze the response stability with respect to the perturbation of influences, as well as to another type of the parametric perturbations of the operator.

STEP 2.1. Perturbation of influences

The possibility of the appearance of kinematic disturbances for a representative volume is due to the fact that during the manufacture of products (or during the experiments), the influences (determined by the boundary conditions of the structure), are not always known with sufficient accuracy. The following perturbed influences are considered:

– for quasi-compression

$$\mathbf{L}_1{}^*(t)=\left(\frac{\alpha(t)}{2}\right)(\mathbf{p}_1\mathbf{p}_1+\mathbf{p}_2\mathbf{p}_2)-\alpha(t)\,\mathbf{p}_3\mathbf{p}_3-\left(\alpha(t)-\dot{\varepsilon}\right)\mathbf{p}_2\mathbf{p}_3; \tag{5}$$

– for shear

$$\mathbf{L}_2{}^*(t)=\left(\frac{\alpha(t)-\dot{\varepsilon}}{2}\right)(\mathbf{p}_1\mathbf{p}_1+\mathbf{p}_2\mathbf{p}_2)-\left(\alpha(t)-\dot{\varepsilon}\right)\,\mathbf{p}_3\mathbf{p}_3-\alpha(t)\,\mathbf{p}_2\mathbf{p}_3. \tag{6}$$

Coincidence of the perturbed influence with the base one corresponds to $\alpha(t)=\dot{\varepsilon}$. The function $\alpha(t)$ that specifies the current "perturbed" strain rate was set in such a way as to provide the "sawtooth" (with random duration and burst height) changes in the components $\mathbf{L}^*(t)$ relative to the components $\mathbf{L}(t)$. The duration of the bursts produced alternatively "up" and "down" (c $\alpha(t)\geq\dot{\varepsilon}$ and $\alpha(t)\leq\dot{\varepsilon}$, respectively) was determined randomly by using a uniform distribution law in the interval from 0 to 10 sec and approximated to a value corresponding to as many steps as necessary for the time integration of the CM. The peak value $\alpha_{\max}$ was $\left(1+\omega\,\delta_{L\_\max}\right)\dot{\varepsilon}$ for the odd bursts and $\left(1-\omega\,\delta_{L\_\max}\right)\dot{\varepsilon}$ for the even bursts, where ω is the random value of a uniform distribution for the segment [0,1], $\delta_{L\_\max}$ is the range of relative variability of the parameter for the current computational experiment. At the beginning time of burst t_{start}, no perturbations occured: $\alpha(t_{start})=\dot{\varepsilon}$. The current value α was taken so that it could change linearly and reach $\alpha_{\max}$ in the middle of the burst and return lineraly to $\alpha=\dot{\varepsilon}$ at the end of the burst.

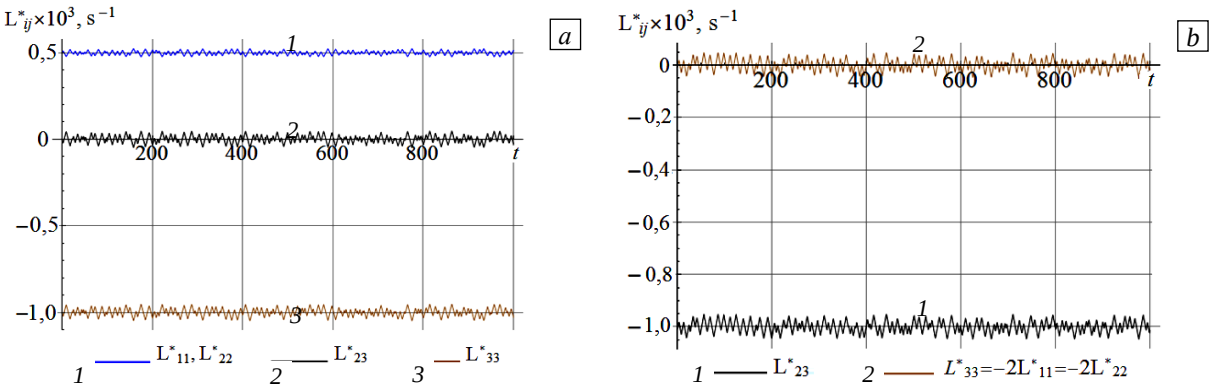

Fig.2. Changes of the nontrivial components $\mathbf{L}^*(t)$ in the randomly selected implementations of computational experiments under the perturbations of influences for quasi-compression (a) and for simple shear (b); $\delta_{L\_\max}=0,05$.

Figure 2 presents the changes in the components of the tensor $\mathbf{L}^*(t)$ in the LCS obtained according to (5) and (6) for some implementations of the computational experiments at $\delta_{L\_\max} = 0,05$.

STEP2.2. Operator perturbation

For the parametric perturbation of the operator, the deviations of the critical shear stresses on slip systems at different times after the initial one were specified. The relevance of this study is due to the fact that some physical processes are stochastic in nature, e.g., the interactions between defect structures at microscale levels, which were taken into account in an effective way in CMs in terms of critical shear stresses forf individual crystallites at the meso-scale (a review of approaches to the formulation of hardening relations is provided in [5]). The practical application of the definition of stability introduced in [28] leads to the problem of calculating the deviation norm of an operator. Due to significant nonlinearity and high dimensionality of the CM, this norm cannot be found analytically, and there are no methods for its numerical calculation; if such a method exists, then its implementation would present a difficulty to researchers because of huge resource intensity.

In the numerical procedure for estimating stability, we used a norm for the perturbed parameters of operator $\left\|\mathbf{\Lambda}_{t\in[0,T]}\right\|_{Q_2^S}$. If only critical stresses are disturbed, then we get $S = NK$, where N is the number of grains, K is the number of crystallographic slip systems (as shown above, $N = 343$, $K = 24$), and the norm takes the form [28]:

$$\left\|\mathbf{\Lambda}_{t\in[0,T]}\right\|_{Q_2^S} = \left(\int_0^T \left\langle \left(\tau_c(t)\right)^2 \right\rangle dt\right)^{1/2}, \tag{7}$$

where $\left\langle \left(\tau_c(t)\right)^2 \right\rangle$ is the squared critical shear stress averaged over all K slip systems in all N crystallites from the sample for the corresponding representative volume. The norm of deviation of operator parameters is defined as

$$\left\|\mathbf{\Lambda}^*_{t\in[0,T]} - \mathbf{\Lambda}_{t\in[0,T]}\right\|_{Q_2^S} = \left(\int_0^T \left\langle \left(\tau_c{}^*(t) - \tau_c(t)\right)^2 \right\rangle dt\right)^{1/2}, \tag{8}$$

where $\left\langle \left(\tau_c{}^*(t) - \tau_c(t)\right)^2 \right\rangle$ is the squared deviation of the critical stresses in the current implementation (averaged over all K slip systems in all N crystallites) from those obtained in the base solution. Transition to (8) for characterizing operator deviations suggests sufficient smoothness of the nonlinear operator of the CM in the vicinity of the solution under study.

The critical stress perturbation was realized in such a way as to provide a "sawtooth" change in the critical stresses in the current implementation $\left\langle \tau_c{}^*(t) \right\rangle$ with respect to $\left\langle \tau_c(t) \right\rangle$, i.e., a change with random duration and burst height. The duration of bursts produced alternatively "up" and "down" was determined randomly by using a uniform distribution law in the interval from 0 to 10 sec. The peak deviation of mean critical stresses, which must be achieved at the burst during the perturbed and nonperturbed calculations, was specified as $\beta = \left\langle \tau_c(t_{start}) \right\rangle \omega\, \delta_{\tau\_\max}$, where $\left\langle \tau_c(t_{start}) \right\rangle$ are the average stresses in the base solution at the starting time of burst t_{start}, ω is the random value from the uniform law of distribution over the segment [0,1], $\delta_{\tau\_\max}$ is the range of relative variability of the parameter from the computational experiment. No perturbation was observed at the instant of time t_{start}.

In the implementation of odd bursts at all steps of the CM integration, the critical stresses for all slip systems of all crystallites (after the CM integration procedure at the time step) increased further

with the same factor so that the deviation of the average critical stresses in the "perturbed" calculation from the values in the basic calculation increased linearly and reached a peak in the middle of the burst. After the peak, the uniform compression of the yield surface was carried out until the average critical stresses in the perturbed solution were equalized with the values obtained in the basic calculation. For even bursts, the compression and subsequent tension of the yield surface were set in a similar way.

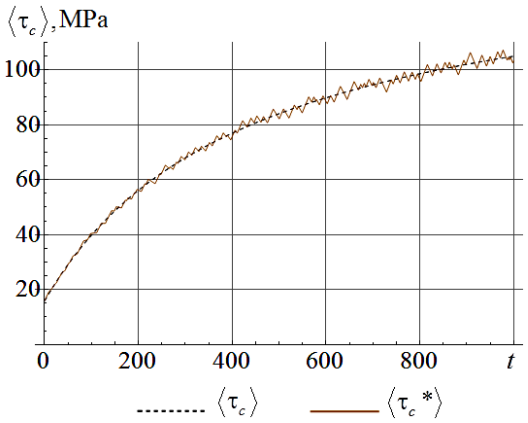

Fig.3. Change in the mean critical stresses in the base calculation with perturbations (randomly selected implementation) at simple shear, $\delta_{\tau\_\max} = 0,05$.

Generally speaking, the stress and yield surface parameters cannot be considered as independent parameters in plasticity models. For example, when the size of the yield polyhedron (there are stresses in the stress space on the polyhedron surface) reduces, it is necessary to correspondingly reduce stresses (the "return mapping" technique often used in numerical procedures for solving plasticity problems); an increase in the size of the yield polyhedron under isothermal conditions occurs due to the increase in stresses. Therefore, due to critical stress perturbations (expansion or contraction of the yield surface of a crystallite), mesostresses also change, which guarantees that the state (elastic or inelastic) of the material will remain unchanged.

For illustration, Figure 3 presents the calculated curves showing the change in the process of deformation of the critical stresses for the mean critical stresses obtained in the basic calculation and in the calculation with perturbations. Note that the character of the deviation of the mean critical stresses (Fig. 3) is more complicated than that of the impact parameters (Fig. 2). This can be explained by the fact that the critical stresses are the IVs of the problem, and the magnitude of this deviation from the basic solution is determined not only by the prescribed perturbation law, but also depends on the values of the perturbed IV established at the time of perturbation, according to the relations of the CM itself.

STEP 3 Schedule of numerical experiments

For implementing the model under basic loads (*STEP 1*), the above-described perturbations of influences and operator (*STEP 2*) were realized at different ranges of relative variability of the parameters $\delta_{L\_\max}$, $\delta_{\tau\_\max}$, according to the calculation schedule given in Table 1.

Table 1. Schedule of computational expriments.

№	Type of experiment	№	Type of experiment
1	Quasi-compression with perturbation $\mathbf{L}(t)$	4	Shear with perturbation $\mathbf{L}(t)$
2	Quasi-compression with perturbation $\tau_c(t)$	5	Shear with perturbation $\tau_c(t)$
3	Quasi-compression with perturbation and $\mathbf{L}(t)$, and $\tau_c(t)$	6	Shear with perturbation and $\mathbf{L}(t)$,and $\tau_c(t)$

STEP 4 Implementation of computational experiments

For each type of the computational experiments (Table 1), 3 series of 50 calculations were carried out with random realization of perturbations in each, and every series referred to certain

ranges of relative variability of the parameters $\delta_{L\_\max}, \delta_{\tau\_\max}$. The results of the calculations with perturbations are denoted by the symbol '*'. Figures 4, 5 present examples that illustrate some of the results of separate computational experiments. Table 2 contains the statistical information obtained after processing a set of results from all implementations.

Figure 4 gives the time curves of largest modulus components of the macrostress tensor constructed using the results of the basic calculations and calculations with perturbations (implementation is taken randomly).

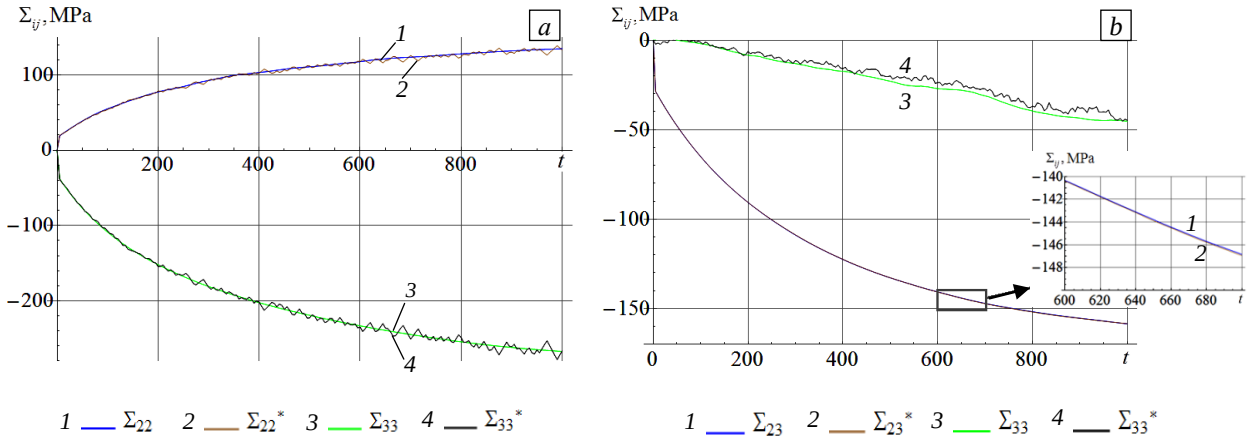

Fig.4. Time variation of the components of the macrostress tensor in the second-type computational experiments with $\delta_{L\_\max} = 0$, $\delta_{\tau\_\max} = 0{,}05$ (critical stress perturbations at quasi-compression) (*a*) and in the forth-type expriments with $\delta_{L\_\max} = 0{,}05$, $\delta_{\tau\_\max} = 0$ (pertrurabations of kinematic influences at shear) (b).

It can be seen from Figure 4 that the perturbed solution is close to the basic one for the perturbations under consideration. In addition, it should be noted that the pole figures obtained in the basic solutions and in the solutions with perturbations are visually almost the same. When critical stresses are perturbed in accordance with the accepted variation law, the changes in all components of the macrostress tensor are significant (Fig. 4a). It is interesting that in the calculations with kinematic influence perturbation (deformation trajectories), the values of the dominant component of the stress tensor are close to the values obtained in the basic calculation (Figure 4b shows that the deviations practically coincide). This can be associated with the description of the mesostress evolution in the CM: with the adopted exponent $m = 83{,}3$ in the viscoplastic law under active loading, the mesostresses (deviator) are near the surface of the yield polyhedron, which is determined by the Schmid criterion [5, 62]. For the perturbations under study, the deformation trajectory remains close to the baseline, and therefore the stress in the stress space for crystallites tends to move in the direction corresponding to an increase in the dominant stress component. At the initial stage, the stresses are located near the faces of the crystallite yield surface (i.e., a convex polyhedron [5]) and the maximum of this stress deviator component is in correspondence with it. During subsequent loading, the yield surface transforms: it expands in the direction of an increase in the dominant component of the stress deviator together with the displacement of the stress in the stress space. Since the values of the maximum accumulated deformation for the dominant component, corresponding to the basic and perturbed options, are close, so the changes in the yield surfaces in this direction for the base and perturbed modes will differ only slightly, which will result in the proximity of the obtained values of the dominant component. At the same time, the face of the yield surface with the maximum value of the dominant stress deviator component can be practically normal to the direction in which the stresses increase, and the perturbations of kinematic influences will manifest themselves in the movement of the stress along this face of the yield surface.

Figure 5 shows typical time dependences of the mesostress tensor components for an individual crystallite, which were plotted based on the same calculated data as those from Fig. 4b. Note that, for the nondominant stress components, the deviations at the macrolevel are smaller due to the averaging of mesostresses over a sufficiently large number (343) of crystallites.

We have calculated the values of the norms [28] :

– deviations of the history of influences $\left\|\mathbf{X}^*_{t\in[0,T]}-\mathbf{X}_{t\in[0,T]}\right\|_{Q_2^m}$, the norm is defined by Riemann integral $\left\|\mathbf{X}_{t\in[0,T]}\right\|_{Q_2^m}=\left(\int_0^T\sum_{i=1}^m\left(X_i(t)\right)^2dt\right)^{1/2}$ in the space $Q_{2\,t\in[0,T]}^m$ of the piecewise continuous vector functions of the dimension m at $t\in[0,T]$ [63], in the calculation performed here $m=9$ (number of the components $\mathbf{L}$);

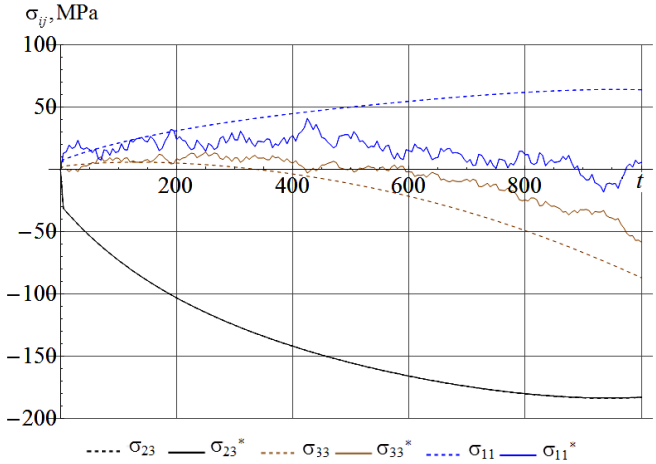

Fig.5. Time variation of the components of the crystallite mesostress tensor during implementation No.1 in the forth-type expriment with $\delta_{L\_\max}=0,05$.

– deviations of the operator parameter according to (8);

– deviations of the solutions $\left\|\mathbf{Y}^*_{t\in[0,T]}-\mathbf{Y}_{t\in[0,T]}\right\|_{C_{L^2}^n}$, the norm is also defined by Riemann integral, but in the space $C_{L^2}^n$ of the continuous vector functions of the dimension n at $t\in[0,T]$; in the calculations $n=9$ (the number of the macrostress tensor components $\mathbf{\Sigma}$).

We note that, in the general case of the analysis of different types of influences, operator parameters, IVs and response, it is necessary to introduce the vectors ($\mathbf{X}$, $\mathbf{\Lambda}$, $\mathbf{Z}$, $\mathbf{Y}$) with subsequent nondimensionalization of the components into characteristic values. In the case under study, due to the uniformity of the components of these vectors, the necessity to do this is absent.

According to the definition formulated in [28], *the base solution will be stable* if, for any $\varepsilon>0$, there are such (defined in the corresponding normalized spaces) neighborhoods of the initial conditions, influences, and operator parameters that (while finding the corresponding perturbed characteristics) the solutions established in terms of the model will be located in the ε-neighborhood of the basic solution.

The stability of the model can be assessed by checking the stability of solutions for different values of the parameters (taken from different subsets of the domain of definition) used to specify the operator and input data (initial conditions and influences) [28]. This article does not present the results of a study of perturbations of the initial conditions. Our previous paper [27] contains the results which confirm the stability of CMs to the perturbations of initial the conditions.

STEP 5. Analysis of the fulfilment of requirements referring to the definition of stability for each basic solution on the set of calculated data

Table 2 contains relative estimates for the norms $\dfrac{\left\|\mathbf{X}^*_{t\in[0,T]}-\mathbf{X}_{t\in[0,T]}\right\|_{Q_2^m}^{\text{об.}}}{\left\|\mathbf{X}_{t\in[0,T]}\right\|_{Q_2^m}}=\Delta_{\mathbf{X}}$, $\dfrac{\left\|\mathbf{\Lambda}^*_{t\in[0,T]}-\mathbf{\Lambda}_{t\in[0,T]}\right\|_{Q_2^S}^{\text{об.}}}{\left\|\mathbf{\Lambda}_{t\in[0,T]}\right\|_{Q_2^S}}=\Delta_{\mathbf{\Lambda}}$ and $\dfrac{\left\|\mathbf{Y}^*_{t\in[0,T]}-\mathbf{Y}_{t\in[0,T]}\right\|_{C_{L^2}^n}^{\text{об.}}}{\left\|\mathbf{Y}_{t\in[0,T]}\right\|_{C_{L^2}^n}}=\Delta_{\mathbf{Y}}$, which were found in different implementations of the computational experiments. For short, these are called relative norms. For the numerical expriments No 3 and No 6, we assumed that $\delta_{L\_\max}=\delta_{\tau\_\max}$, and therefore, to denote

the range of their relative variability, further we introduce the same notion, δ , further for all parameters. For each δ ($\delta = 0,01;\ 0,03;\ 0,05$), 50 points are plotted on all curves (150 points in all); every point corresponds to the implementation of one computational experiment for which $\mathbf{X}^*_{t\in[0,T]}$, $\mathbf{\Lambda}^*_{t\in[0,T]}$, $\mathbf{Y}^*_{t\in[0,T]}$ are defined to calculate the above mentioned norms. Note that, in the CM, the evolution of IVs is shown for 343 grains; some particular results are given in Figures 4 and 5.

Strictly speaking, the norm of deviation of the parameters of operator (8) under the perturbations of influences is not an estimate of the norm of deviation of the operator [28]. In this case, the nonperturbed and perturbed critical stresses are investigated for different input data (with different histories of influences). However, it seems necessary to consider joint perturbations in the analysis of stability; the norm (8) can be interpreted literally as an integral assessment of the deviations of the history of changes in the IVs obtained by the CM. If the smaller $\Delta_{\mathbf{\Lambda}}$ are in the correspondence with the smaller $\Delta_{\mathbf{Y}}$, then this can be regarded as indirect evidence of the stability of the solution with respect to the investigated perturbations of operator.

The results shown in Table 2 can be represented as the dependences of the relative deviation of the response on the relative deviation of the history of influences and the relative deviation of operator. For illustration, the corresponding data obtained in the series of experiments No. 6 are given in Fig.6.

Based on the results of the calculations, we can suggest that the CM has a noticeable sensitivity to the perturbations of both kinematic influences and critical stresses, which requires careful consideration of the issues related to describing geometric nonlinearity and formulating hardening laws (kinetic equations for critical stresses). Note that the joint perturbation of parameters leads (according to the average estimate) to a greater deviation of the response.

Table 2. Numerical estimates for relative norms at different parameters of the relative perturbation δ (mathematical expectation and standard deviation of relative norms).

<table>
<tr><th>$\Delta_{\mathbf{X}}$</th><th>$\Delta_{\mathbf{\Lambda}}$</th><th>$\Delta_{\mathbf{Y}}$</th></tr>
<tr><td colspan="3">1st type experiments: quasi-compression with perturbation $\mathbf{L}(t)$</td></tr>
<tr><td> 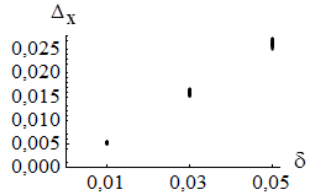

<table>
<tr><td>M</td><td>5,27·10^-3</td><td>1,59·10^-2</td><td>2,63·10^-2</td></tr>
<tr><td>S</td><td>1,17·10^-4</td><td>4,08·10^-4</td><td>5,48·10^-4</td></tr>
</table></td><td>ignored</td><td> 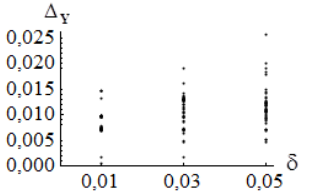

<table>
<tr><td>M</td><td>8,36·10^-3</td><td>1,09·10^-2</td><td>1,15·10^-2</td></tr>
<tr><td>S</td><td>2,53·10^-3</td><td>3,22·10^-3</td><td>3,8·10^-3</td></tr>
</table></td></tr>
<tr><td colspan="3">2d type experiments: quasi-compression with perturbation $\tau_c(t)$</td></tr>
<tr><td>0</td><td> 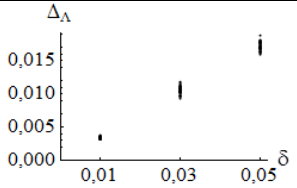

<table>
<tr><td>M</td><td>3,43·10^-3</td><td>1,05·10^-2</td><td>1,72·10^-2</td></tr>
<tr><td>S</td><td>1,57·10^-4</td><td>5,66·10^-4</td><td>6,14·10^-4</td></tr>
</table></td><td> 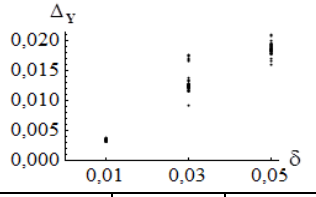

<table>
<tr><td>M</td><td>3,44·10^-3</td><td>1,29·10^-2</td><td>1,86·10^-2</td></tr>
<tr><td>S</td><td>1,53·10^-4</td><td>1,72·10^-3</td><td>8,48·10^-4</td></tr>
</table></td></tr>
<tr><td colspan="3">3d type experiments: quasi-compression with perturbation and $\mathbf{L}(t)$, and $\tau_c(t)$</td></tr>
</table>

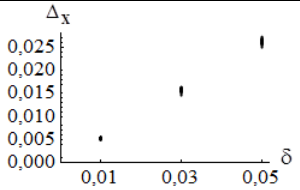

M	$5{,}28\cdot10^{-3}$	$1{,}58\cdot10^{-2}$	$2{,}62\cdot10^{-2}$
S	$1{,}42\cdot10^{-4}$	$3{,}67\cdot10^{-4}$	$4{,}78\cdot10^{-4}$

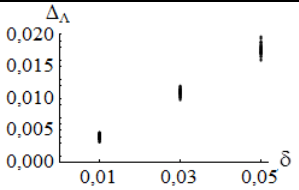

M	$4{,}01\cdot10^{-3}$	$1{,}10\cdot10^{-2}$	$1{,}77\cdot10^{-2}$
S	$4{,}02\cdot10^{-4}$	$5{,}22\cdot10^{-4}$	$8{,}04\cdot10^{-4}$

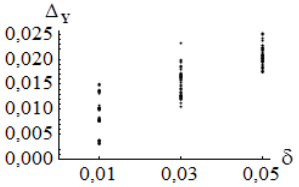

M	$9{,}04\cdot10^{-3}$	$1{,}12\cdot10^{-2}$	$2{,}07\cdot10^{-2}$
S	$3{,}6\cdot10^{-3}$	$2{,}73\cdot10^{-3}$	$1{,}95\cdot10^{-3}$

4th type experiments: shear with perturbation $\mathbf{L}(t)$

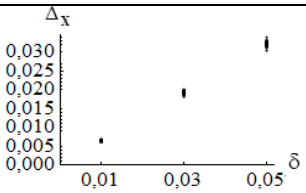

M	$6{,}43\cdot10^{-3}$	$1{,}93\cdot10^{-2}$	$3{,}22\cdot10^{-2}$
S	$1{,}6\cdot10^{-4}$	$4{,}47\cdot10^{-4}$	$6{,}13\cdot10^{-4}$

Не рассматривалось

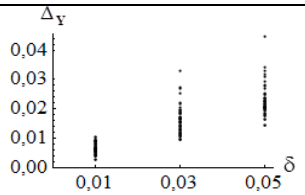

M	$6{,}56\cdot10^{-3}$	$1{,}61\cdot10^{-2}$	$2{,}27\cdot10^{-2}$
S	$1{,}9\cdot10^{-3}$	$4{,}96\cdot10^{-3}$	$5{,}43\cdot10^{-3}$

5th type experiments: shear with perturbation $\tau_c(t)$

0

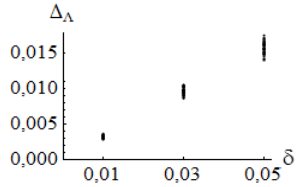

M	$3{,}19\cdot10^{-3}$	$9{,}6\cdot10^{-3}$	$1{,}56\cdot10^{-2}$
S	$1{,}58\cdot10^{-4}$	$4{,}7\cdot10^{-4}$	$8{,}18\cdot10^{-4}$

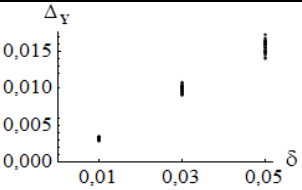

M	$3{,}19\cdot10^{-3}$	$9{,}96\cdot10^{-3}$	$1{,}57\cdot10^{-2}$
S	$1{,}55\cdot10^{-4}$	$4{,}61\cdot10^{-4}$	$7{,}88\cdot10^{-4}$

6th type experiments: shear with perturbation and $\mathbf{L}(t)$, and $\tau_c(t)$

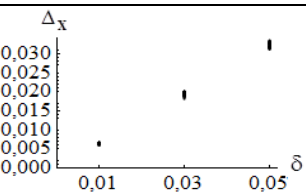

M	$6{,}39\cdot10^{-3}$	$1{,}93\cdot10^{-2}$	$3{,}23\cdot10^{-2}$
S	$1{,}68\cdot10^{-4}$	$4{,}4\cdot10^{-4}$	$6{,}05\cdot10^{-4}$

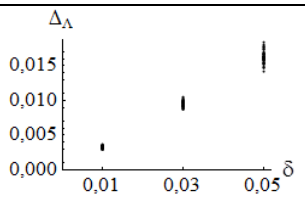

M	$3{,}29\cdot10^{-3}$	$9{,}54\cdot10^{-3}$	$1{,}62\cdot10^{-2}$
S	$1{,}89\cdot10^{-4}$	$4\cdot10^{-4}$	$8{,}98\cdot10^{-4}$

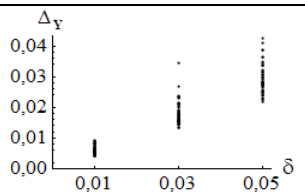

M	$6{,}3\cdot10^{-3}$	$1{,}82\cdot10^{-2}$	$2{,}94\cdot10^{-2}$
S	$1{,}39\cdot10^{-3}$	$3{,}89\cdot10^{-3}$	$4{,}87\cdot10^{-3}$

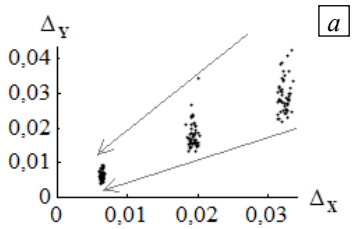

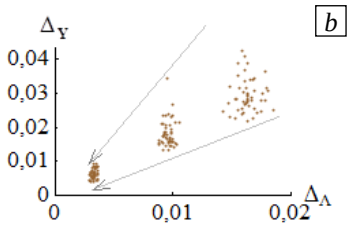

Fig.6. Change of Δ_Y in relation to Δ_X (*a*) and Δ_Λ (b), determined in the series of experiment No 6; solid lines show the ranges of the results obtained; as the norms of deviation of influences and operator parameters decrease, the norm of deviation of the response from that obtained during the base calculation also decreases.

The analysis of the stability of the basic solutions led to the conclusion that for small perturbations there occur small deviations of the solutions and this, according to the criterion [28], indicates the stability of the model. When the parameter perturbation range decreases, the values of all relative norms (influences, operator and response) also decrease. In other words, with a decrease in the norm of deviations of influences and a decrease in the norm of operator perturbations, the norm of deviations of the response also decreases, which provides evidence to the stability of the CM with respect to the perturbations under consideration.

In should be noted that, for individual crystallites, the deviations of mesostresses (IVs in the CM) can exceed the mean values for the representative volume and can increase with time under loading conditions (Fig. 5). This is due to the different motion of the stress in the stress space (generated by the perturbation) on the yield surface; the surface subjected to anisotropic hardening is also transformed in a different way. However, the deviations of macrostresses observed in this case are much smaller due to averaging over a large number of crystallites (Fig.4b).

It would seem necessary, in this respect, to pay attention to the effects caused by the CM structure and the type of applied kinematic influences. The difference in the relative norm of deviation of the mean critical stresses in the experiments of the second and third types (Table 2) is associated with the change of these stresses (indicated above) due to the perturbations of influences. The stress in the stress space (SSS) move on the yield surface, and the implementation of quasi-compression requires that they move between the high-order yield surface vertices (provided that the Schmid criterion is fulfilled on the sixth or eighth systems [64, 65]). After the SSS reaches the adjacent vertex, large perturbations are required to return it to the initial point (that is the reason why, at the given level of perturbations, the return is rarely realized). The same effect explains the decrease in the dispersion of the response deviation data and the separation of the points (at some values of δ) into clusters in experiments of the second and third types. At shear, the tendency of the SSSs to high-order vertices is not necessary. For example, at a certain orientation of the crystallite, the shear can be realized due to the motion of dislocations in only one active slip system, when the SSS is on the face of the yield surface. In this situation, at relatively small perturbations, the SSS can easily go to the edges and/or vertices of the yield surface and then return to the initial position. For this reason, in Table 2, there are no significant differences in the deviation of the mean critical stresses in the experiments of the fifth and sixth types.

STEP 6. Analysis of unstable solutions (if they have been established)

In the series of the calculations carried out in this study, the instability of solutions has not been revealed. This is largely because of the uniformity of the distribution of crystallite orientations (the initial plastic properties at the macrolevel are close to isotropic); there are no pronounced edges on the relative yield surface at the macrolevel. At the same time, the analysis of the results from Table 2 has revealed the presence of some points with significantly larger values of the relative norms of response deviations in comparison with the average values obtained in the same experiment. This is due to the fact that, under the prescribed perturbations of influences and model operator, a significant change in the response associated with a change in the motion of the SSSs on the yield surface was observed for a larger number of crystallites.

4. Conclusion

Due to the stochastic character of the properties of the material (including those at the lowest scale levels) and the influences produced by the boundary conditions, the analysis of the stability of solutions (the history of changes in responses) with respect to the perturbations of input data and the perturbations of operator obtained using constitutive material models is of great relevance .

In this connection, the approach previously developed by the authors [28] was applied to investigate the stability of constitutive models. The study included the analysis of different perturbations of the initial conditions, the history of influences and the operator, as well as the determination of the norms of deviation of the corresponding solutions from the baseicones.

The results obtained for the two-level model of the polycrystalline FCC metal demonstrated the stability of this model and its applicability for describing technological processes of thermomechanical treatment.

This work was supported by the Russian Science Foundation (grant No. 17-19-01292).

References

1. McDowell D.L. A perspective on trends in multiscale plasticity. *Int. J. Plast.*, 2010, vol. 26, pp. 1280-1309. https://doi.org/10.1016/j.ijplas.2010.02.008
2. Roters F., Eisenlohr P., Hantcherli L., Tjahjanto D.D., Bieler T.R., Raabe D. Overview of constitutive laws, kinematics, homogenization and multiscale methods in crystal plasticity finite-element modeling: Theory, experiments, applications. *Acta Materialia*, 2010, vol. 58, pp. 1152-1211. https://doi.org/10.1016/j.actamat.2009.10.058
3. Diehl M. Review and outlook: mechanical, thermodynamic, and kinetic continuum modeling of metallic materials at the grain scale. *MRS Communications*, 2017, vol. 7, pp. 735-746. https://doi.org/10.1557/mrc.2017.98
4. Beyerlein I., Knezevic M. Review of microstructure and micromechanism-based constitutive modeling of polycrystals with a low-symmetry crystal structure. *J. Mater. Res.*, 2018, vol. 33, pp. 3711-3738. https://doi.org/10.1557/jmr.2018.333
5. Trusov P.V., Shveykin A.I. *Mnogourovnevyye modeli mono- i polikristallicheskikh materialov: teoriya, algoritmy, primery primeneniya* [Multilevel models of mono- and polycrystalline materials: theory, algorithms, examples of application]. Novosibirsk, Izd-vo SO RAN, 2019. 605 p. https://doi.org/10.15372/MULTILEVEL2019TPV
6. Trusov P.V., Shveikin A.I., Kondratyev N.S., Yants A.Yu. Multilevel models in physical mesomechanics of metals and alloys: results and prospects. *Phys. Mesomech.*, 2020, vol. 23, no. 6, pp. 33-62. https://doi.org/10.24411/1683-805X-2020-16003
7. Trusov P.V. Classical and multi-level constitutive models for describing the behavior of metals and alloys: Problems and Prospects (as a matter for discussion). *Mech. Solids*, 2021, vol. 56, pp. 55-64. https://doi.org/10.3103/S002565442101012X
8. Truesdell C. *A first course in rational continuum mechanics*. USA, Maryland, Baltimore, The Johns Hopkins University, 1972. 304 p.
9. Astarita G., Marrucci G. *Principles of non-Newtonian fluid mechanics*. McGraw-Hill, 1974. 296 p.
10. Guo Y.B., Wen Q., Horstemeyer M.F. An internal state variable plasticity-based approach to determine dynamic loading history effects on material property in manufacturing processes. *Int. J. Mech. Sci.*, 2005, vol. 47, pp. 1423-1441. https://doi.org/10.1016/j.ijmecsci.2005.04.015
11. Maugin G.A. The saga of internal variables of state in continuum thermos-mechanics (1893-2013). *Mech. Res. Comm.*, 2015, vol. 69, pp. 79-86. https://doi.org/10.1016/j.mechrescom.2015.06.009
12. Rice J.R. Inelastic constitutive relations for solids: An internal-variable theory and its application to metal plasticity. *J. Mech. Phys. Solid.*, 1971, vol. 19, pp. 433-455. https://doi.org/10.1016/0022-5096(71)90010-X
13. Mandel J. Equations constitutives et directeurs dans les milieux plastiques et viscoplastiquest. *Int. J. Solid. Struct.*, 1973, vol. 9, pp. 725-740. https://doi.org/10.1016/0020-7683(73)90120-0
14. Aravas N. Finite elastoplastic transformations of transversely isotropic metals. *Int. J. Solids Struct.*, 1992, vol. 29, pp. 2137-2157. https://doi.org/10.1016/0020-7683(92)90062-X
15. Aravas N. Finite-strain anisotropic plasticity and the plastic spin. *Modelling Simul. Mater. Sci. Eng.*, 1994, vol. 2, pp. 483-504. https://doi.org/10.1088/0965-0393/2/3A/005
16. Dafalias Y.F. On multiple spins and texture development. Case study: kinematic and orthotropic hardening. *Acta Mechanica*, 1993, vol. 100, pp. 171-194. https://doi.org/10.1007/BF01174788
17. Trusov P.V. (ed.) *Vvedeniye v matematicheskoye modelirovaniye* [Introduction to mathematical modeling]. Moscow, Logos, 2007. 440 p.
18. Sobol' I.M. Ob otsenke chuvstvitel'nosti nelineynykh matematicheskikh modeley [On the estimation of the sensitivity of nonlinear mathematical models]. *Matem. modelirovaniye – Mathematical Models and Computer Simulations*, 1990, vol. 2, no. 1, pp. 112-118.
19. Archer G.E.B., Saltelli A., Sobol I.M. Sensitivity measures, ANOVA-like techniques and the use of bootstrap. *J. Stat. Comput. Simulat.*, 1997, vol. 58, pp. 99-120. https://doi.org/10.1080/00949659708811825
20. Saltelli A., Tarantola S., Chan K.P.-S. A quantitative model-independent method for global sensitivity analysis of model output. *Technometrics*, 1999, vol. 41, pp. 39-56. https://doi.org/10.1080/00401706.1999.10485594
21. Sobol I.M. Global sensitivity indices for the investigation of nonlinear mathematical models. *Matem. modelirovaniye – Mathematical Models and Computer Simulations*, 2005, vol. 17, no. 9, pp. 43-52.
22. Saltelli A., Ratto M., Andres T., Campolongo F., Cariboni J., Gatelli D., Saisana M., Tarantola S. *Global sensitivity analysis. The Primer*. John Wiley & Sons Ltd., 2008. 292 p.
23. Yang Z., Elgamal A. Application of unconstrained optimization and sensitivity analysis to calibration of a soil constitutive model. *Int. J. Numer. Anal. Meth. Geomech.*, 2003, vol. 27, pp. 1277-1297. https://doi.org/10.1002/nag.320

24. Qu J., Xu B., Jin Q. Parameter identification method of large macro-micro coupled constitutive models based on identifiability analysis. *CMC*, 2010, vol. 20, pp. 119-157. https://doi.org/10.3970/cmc.2010.020.119
25. Shutov A.V., Kaygorodtseva A.A. Parameter identification in elasto-plasticity: distance between parameters and impact of measurement errors. *ZAMM*, 2019, vol. 99, e201800340. https://doi.org/10.1002/zamm.201800340
26. Kotha S., Ozturk D., Ghosh S. Parametrically homogenized constitutive models (PHCMs) from micromechanical crystal plasticity FE simulations, part I: Sensitivity analysis and parameter identification for titanium alloys. *Int. J. Plast.*, 2019, vol. 120, pp. 296-319. https://doi.org/10.1016/j.ijplas.2019.05.008
27. Shveykin A.I., Sharifullina E.R., Trusov P.V., Pushkov D.A. About estimation of sensitivity of statistical multilevel polycrystalline metal models to parameter variations. *Vychisl. mekh. splosh. sred – Computational Continuum Mechanics*, 2018, vol. 11, no. 2, pp. 214-231. https://doi.org/10.7242/1999-6691/2018.11.2.17
28. Shveykin A.I., Trusov P.V., Romanov K.A. An approach to numerical estimating the stability of multilevel constitutive models. *Vychisl. mekh. splosh. sred – Computational Continuum Mechanics*, 2021, vol. 14, no. 1, pp. 61-76. https://doi.org/10.7242/1999-6691/2021.14.1.6
29. Lyapunov A.M. *Obshchaya zadacha ob ustoychivosti dvizheniya* [General problem of motion stability]. Moscow, Leningrad, Gosudarstvennoye izd-vo tekhniko-teoreticheskoy literatury, 1950. 470 p.
30. Barbashin E.A. *Vvedeniye v teoriyu ustoychivosti* [Introduction to the theory of stability]. Moscow, Nauka, 1967. 223 p.
31. Demidovich B.P. *Lektsii po matematicheskoy teorii ustoychivosti* [Lectures on the mathematical theory of stability]. Moscow, Nauka, 1967. 472 p.
32. Berge P., Pomeau Y., Vidal C. *L'ordre dans le chaos. Vers une approche déterministe de la turbulence* [Order in chaos. On a deterministic approach to turbulence]. Hermann, Editeurs des sciences et des arts, 1988. 353 p.
33. Lyapunov A.M. The general problem of the stability of motion. *Int. J. Contr.*, 1992, vol. 55, pp. 531-534. https://doi.org/10.1080/00207179208934253
34. Precup R.-E., Tomescu M.-L., Preitl St. Fuzzy logic control system stability analysis based on Lyapunov's direct method. *International Journal of Computers, Communications & Control*, 2009, vol. 4, pp. 415-426. https://doi.org/10.15837/ijccc.2009.4.2457
35. Li Y., Chen Y.Q., Podlubny I. Stability of fractional-order nonlinear dynamic systems: Lyapunov direct method and generalized Mittag–Leffler stability. *Comput. Math. Appl.*, 2010, vol. 59, pp. 1810-1821. https://doi.org/10.1016/j.camwa.2009.08.019
36. Aguila-Camacho N., Duarte-Mermoud M.A., Gallegos J.A. Lyapunov functions for fractional order systems. *Comm. Nonlinear Sci. Numer. Simulat.*, 2014, vol. 19, pp. 2951-2957. https://doi.org/10.1016/j.cnsns.2014.01.022
37. Georgievskii D.V., Kvachev K.V. The Lyapunov–Movchan method in problems of the stability of flows and deformation processes. *J. Appl. Math. Mech.*, 2014, vol. 78, pp. 621-633. https://doi.org/10.1016/j.jappmathmech.2015.04.010
38. Habraken A.M. Modelling the plastic anisotropy of metals. *Arch. Computat. Methods Eng.*, 2004, vol. 11, pp. 3-96. https://doi.org/10.1007/BF02736210
39. Van Houtte P. Crystal plasticity based modelling of deformation textures. *Microstructure and Texture in Steels*, ed. A. Haldar, S. Suwas, D. Bhattacharjee. Springer, 2009. P. 209-224. https://doi.org/10.1007/978-1-84882-454-6_12
40. Zhang K., Holmedal B., Hopperstad O.S., Dumoulin S., Gawad J., Van Bael A., Van Houtte P. Multi-level modelling of mechanical anisotropy of commercial pure aluminium plate: Crystal plasticity models, advanced yield functions and parameter identification. *Int. J. Plast.*, 2015, vol. 66, pp. 3-30. https://doi.org/10.1016/j.ijplas.2014.02.003
41. Lebensohn R.A., Ponte Castañeda P., Brenner R., Castelnau O. Full-field vs. homogenization methods to predict microstructure–property relations for polycrystalline materials. *Computational Methods for Microstructure-Property Relationships*, ed. S. Ghosh, D. Dimiduk. Springer, 2011. P. 393-441. https://doi.org/10.1007/978-1-4419-0643-4_11
42. Trusov P.V., Shveykin A.I., Nechaeva E.S., Volegov P.S. Multilevel models of inelastic deformation of materials and their application for description of internal structure evolution. *Phys. Mesomech.*, 2012, vol. 15, pp. 155-175. https://doi.org/10.1134/S1029959912020038
43. Pozdeyev A.A., Trusov P.V., Nyashin Yu.I. *Bol'shiye uprugoplasticheskiye deformatsii: teoriya, algoritmy, prilozheniya* [Large elastoplastic deformations: theory, algorithms, applications]. Moscow, Nauka, 1986. 232 p.
44. Levitas V.I. *Bol'shiye uprugoplasticheskiye deformatsii materialov pri vysokom davlenii* [Large elastoplastic deformations of materials at high pressure]. Kiev, Naukova dumka, 1987. 232 p.
45. Kondaurov V.I., Nikitin L.V. *Teoreticheskiye osnovy reologii geomaterialov* [Theoretical foundations of geomaterial rheology]. Moscow, Nauka, 1990. 207 p.
46. Korobeynikov S.N. *Nelineynoye deformirovaniye tverdykh tel* [Nonlinear deformation of solids]. Novosibirsk, Izd-vo SO RAN, 2000. 262 p.
47. Rogovoy A.A. *Formalizovannyy podkhod k postroyeniyu modeley mekhaniki deformiruyemogo tverdogo tela. Ch. 1. Osnovnyye sootnosheniya mekhaniki sploshnykh sred* [A formalized approach to the construction of models of solid mechanics. Part 1. Basic relations of continuum mechanics]. Moscow, Izd-vo IKI, 2021. 288 p.
48. Markin A.A., Sokolova M.Yu. *Termomekhanika uprugoplasticheskogo deformirovaniya* [Thermomechanics of elastoplastic deformation]. Moscow, Fizmatlit, 2013. 319 p.

49. Brovko G.L. *Opredelyayushchiye sootnosheniya mekhaniki sploshnoy sredy: razvitiye matematicheskogo apparata i osnov obshchey teorii* [Constitutive relations of continuum mechanics: Development of the mathematical apparatus and foundations of the general theory]. Moscow, Nauka, 2017. 432 p.
50. Trusov P.V., Shveykin A.I., Yanz A.Yu. Motion decomposition, frame-indifferent derivatives, and constitutive relations at large displacement gradients from the viewpoint of multilevel modeling. *Phys. Mesomech.*, 2017, vol. 20, pp. 357-376. https://doi.org/10.1134/S1029959917040014
51. Trusov P.V., Shveykin A.I. On motion decomposition and constitutive relations in geometrically nonlinear elastoviscoplasticity of crystallites. *Phys. Mesomech.*, 2017, vol. 20, pp. 377-391. https://doi.org/10.1134/S1029959917040026
52. Trusov P.V., Shveykin A.I., Kondratev N.S. Multilevel metal models: formulation for large displacements gradients. *Nanoscience and Technology: An International Journal*, 2017, vol. 8, pp. 133-166. https://doi.org/10.1615/NanoSciTechnolIntJ.v8.i2.40
53. Anand L. Single-crystal elasto-viscoplasticity: application to texture evolution in polycrystalline metals at large strains. *Comput. Meth. Appl. Mech. Eng.*, 2004, vol. 93, pp. 5359-5383. https://doi.org/10.1016/j.cma.2003.12.068
54. Trusov P.V., Sharifullina E.R., Shveykin A.I. Multilevel model for the description of plastic and superplastic deformation of polycristalline materials. *Phys. Mesomech.*, 2019, vol. 22, pp. 402-419. https://doi.org/10.1134/S1029959919050072
55. Shveykin A., Trusov P., Sharifullina E. Statistical crystal plasticity model advanced for grain boundary sliding description. *Crystals*, 2020, vol. 10(9), 822. https://doi.org/10.3390/cryst10090822
56. Estrin Y., Tóth L.S., Molinari A., Bréchet Y. A dislocation-based model for all hardening stages in large strain deformation. *Acta Mater.*, 1998, vol. 46, pp. 5509-5522. https://doi.org/10.1016/S1359-6454(98)00196-7
57. Staroselsky A., Anand L. Inelastic deformation of polycrystalline face centered cubic materials by slip and twinning. *J. Mech. Phys. Solid.*, 1998, vol. 46, pp. 671-696. https://doi.org/10.1016/S0022-5096(97)00071-9
58. Kalidindi S.R. Modeling anisotropic strain hardening and deformation textures in low stacking fault energy FCC metals. *Int. J. Plast.*, 2001, vol. 17, pp. 837-860. https://doi.org/10.1016/S0749-6419(00)00071-1
59. Beyerlein I.J., Tome C.N. A dislocation-based constitutive law for pure Zr including temperature effects. *Int. J. Plast.*, 2008, vol. 24, pp. 867-895. https://doi.org/10.1016/j.ijplas.2007.07.017
60. Bronkhorst C.A., Kalidindi S.R., Anand L. Polycrystalline plasticity and the evolution of crystallographic texture in FCC metals. *Phil. Trans. Math. Phys. Eng. Sci.*, 1992, vol. 341, pp. 443-477. https://doi.org/10.1098/rsta.1992.0111
61. Harder J. FEM-simulation of the hardening behavior of FCC single crystals. *Acta Mechanica*, 2001, vol. 150, pp. 197-217. https://doi.org/10.1007/BF01181812
62. Shveikin A.I., Sharifullina E.R. Analysis of constitutive relations for intragranular dislocation sliding description within two-level elasto-viscoplastic model of FCC-polycrystals. *Vestnik Tambovskogo universiteta. Seriya Estestvennyye i tekhnicheskiye nauki – Tambov University Reports. Series: Natural and Technical Sciences*, 2013, vol. 18, no. 4-2, pp. 1665-1666.
63. Trenogin V.A. *Funktsional'nyy analiz* [Functional analysis]. Moscow, Nauka, 1980. 495 p.
64. Rocks U.F., Canova G.R., Jonas J.J. Yield vectors in f.c.c. crystals. *Acta metall.*, 1983, vol. 31, pp. 1243-1252. https://doi.org/10.1016/0001-6160(83)90186-4
65. Kuhlman-Wilsdorf D., Kulkarni S.S., Moore J.T., Starke E.A. (Jr.) Deformation bands, the LEDS theory, and their importance in texture development: Part I. Previous evidence and new observations. *Metall. Mater. Trans. A*, 1999, vol. 30, pp. 2491-2501. https://doi.org/10.1007/s11661-999-0258-7

The authors declare no conflict of interests.

The original paper was received on 28.03.2021 and published in Russian on 14.04.2021.